

PCAF-mediated acetylation of transcriptional factor HOXB9 suppresses lung adenocarcinoma progression by targeting oncogenic protein JMJD6

Junhu Wan^{1,†}, Weizhi Xu^{1,†}, Jun Zhan¹, Ji Ma¹, Xueying Li¹, Yuping Xie², Jiadong Wang³, Wei-guo Zhu⁴, Jianyuan Luo⁵ and Hongquan Zhang^{1,*}

¹Department of Anatomy, Histology and Embryology, Key Laboratory of Carcinogenesis and Translational Research (Ministry of Education), and State Key Laboratory of Natural and Biomimetic Drugs, Peking University Health Science Center, Beijing 100191, China, ²School of Life Sciences, Tsinghua University, Beijing 100084, China, ³Department of Radiation Medicine, Peking University Health Science Center, Beijing 100191, China, ⁴Department of Biochemistry and Molecular Biology, Peking University Health Science Center, Beijing 100191, China and ⁵Department of Medical Genetics, Peking University Health Science Center, Beijing 100191, China

Received June 16, 2016; Revised August 31, 2016; Accepted September 03, 2016

ABSTRACT

HOXB9 is a homeobox domain-containing transcription factor, playing an important role in embryonic development and cancer progression. However, the precise post-translational modifications (PTMs) of HOXB9 and the corresponding roles are unclear. Here, we report that acetyltransferase p300/CBP-associated factor (PCAF) interacts with and acetylates HOXB9 both *in vivo* and *in vitro*. Conversely, the acetylation of HOXB9 can be reversed by deacetylase SIRT1. Furthermore, we found that HOXB9 is acetylated at lysine 27 (AcK27). Functionally, in contrast to the wild type HOXB9, AcK27-HOXB9 decreased its capacity in promoting lung cancer cell migration and tumor growth in mice. Mechanistically, AcK27-HOXB9 suppresses the transcription of its target gene Jumonji domain-containing protein 6 (JMJD6) by direct occupying the promoter of JMJD6 gene. For clinical relevance, elevated HOXB9 acetylation at K27 predicts a better prognosis in lung adenocarcinoma patients. Taken together, we identified the first PTM of HOXB9 by demonstrating that HOXB9 can be acetylated and AcK27-HOXB9 counteracts the role of the wild-type HOXB9 in regulating lung adenocarcinoma progression.

INTRODUCTION

The HOX genes, belonging to homeobox superfamily, share a highly conserved 61-amino acids homeobox domain and are essential in embryonic development. In mammals, HOX

gene family consists of four clusters (HOXA, B, C and D) and 39 members in total (1–3). HOX proteins function as monomers or homodimers to directly regulate the transcription of downstream targets, controlling multiple functions including apoptosis, differentiation, cell motility and angiogenesis (4–8). In particular, HOXB9 as a member of HOX B genes cluster has been reported to function in the specification of thoracic skeletal elements and mammary gland development (9,10). Chen et al reported that in response to pregnancy, HOXB9 together with HOXA9 and HOXD9 triple-mutant female mice showed defective expansion and differentiation of the mammary gland ductal system, causing failure in the production of milk (10).

In addition to its crucial roles in development, HOXB9 was also found to be deeply involved in numerous human cancers. HOXB9 was reported to be frequently overexpressed in invasive human breast cancer, and promotes epithelial to mesenchymal transition (EMT) (6,11,12). Moreover, upregulation of HOXB9 in lung adenocarcinoma patients predicts poor outcomes (13). However, decreased expression of HOXB9 showed poor overall survival in colon adenocarcinoma, pancreatic ductal adenocarcinoma or gastric carcinoma patients, displaying an opposite role in cancer progression (14–17). The diverse roles of HOXB9 in different cancer types suggest that the mechanism underlying HOXB9 in cancer progression remains complicated. Furthermore, it remains unclear how HOXB9 itself is being precisely regulated during cancer progression. It has been reported that activator E2F3 and repressor BMI1/PRC1 can mediate the expression of HOXB9 in Hodgkin lymphoma cell line (18). HOXB9 is also a direct transcriptional target of the Wnt/TCF4 pathway in lung cancer (19). In breast cancer, E2F1 was found to bind to the upstream reg-

*To whom correspondence should be addressed. Tel: +86 10 82802424; Fax: +86 10 82802424; Email: Hongquan.Zhang@bjmu.edu.cn

†These authors contributed equally to this work as first authors.

ulatory elements of HOXB9 to form an E2F1-HOXB9 circuit to regulate breast cancer progression (20). Moreover, FAT10, an ubiquitin-like protein is able to regulate HOXB9 expression through the β -catenin/TCF4 pathway in hepatocellular carcinoma (21). However, these opposite roles of HOXB9 may not simply be explained by the protein level of HOXB9 in cells. Other mechanisms for the role of HOXB9 might be existed. So far, there is no report about the post-translational modifications (PTMs) on HOXB9 regulation.

Protein acetylation was firstly found in histone lysine residues. Acetylation in histones was found to mainly regulate gene transcription (22,23). Non-histone protein acetylation, such as p53, STAT3 and EZH2, also have been reported to play important roles in diverse physiological processes (24–28). In this report, we demonstrated that HOXB9 interacts with and is acetylated by acetyltransferase p300/CBP-associated factor (PCAF). As an alternative mechanism we found that acetylated HOXB9 decreased its ability in promotion of lung cancer progression by directly regulating JMJD6 gene expression.

MATERIALS AND METHODS

Cell culture and inhibitors

The human embryonic kidney cell line HEK-293T and human lung adenocarcinoma cell line H1299 were cultured in DMEM and RPMI1640 respectively, supplemented with 10% fetal bovine serum, 100 units/ml penicillin and 100 mg/ml streptomycin at 37°C with 5% (v/v) CO₂. The HDAC inhibitor TSA and class III sirtuin (SIRT) inhibitor nicotinamide were all purchased from Sigma.

Constructs and antibodies

To generate the FLAG tagged HOXB9, the sequence of full-length HOXB9 cDNA was amplified by PCR and subcloned into 3×FLAG vector (Sigma). The FLAG-HOXB9 and MBP-HOXB9 mutants were generated by the QuikChange Site-Directed Mutagenesis Kit (Stratagene). The following antibodies used in the experiments: Acetylated-Lysine and PCAF (Cell Signaling Technology; Catalogue #9441 and #3378, respectively), HOXB9 and JMJD6 (Santa Cruz; sc-398500, sc-133671 and sc-28348 respectively), SIRT1 and SIRT2 (abcam). FLAG and HA (Sigma F1804 and H3663). The rabbit polyclonal antibodies recognizing the acetylated HOXB9 K27 were produced with a synthetic acetylated peptide: ERIK-TPP(AcK)RPGGRR (Kang Wei Shi Ji, Beijing, China).

Co-immunoprecipitation and GST pull-down assays

Cells were lysed in NP40 buffer (50 mM Tris-HCl, pH 7.4, 150 mM NaCl, 1% NP-40, 1 mM EDTA, 10 mM sodium butyrate) containing protease inhibitors for Co-immunoprecipitation and Western blot analysis. For the GST pull-down assays, the cellular supernatants were pre-cleared with Glutathione-Sepharose 4B beads (GE Healthcare), and incubated with beads containing GST fusion proteins. The pull down complex were boiled in SDS-PAGE loading buffer and analysed by Western blot.

In vitro acetylation assay

The *in vitro* acetylation assay was performed from the method published previously (27).

Cell proliferation, migration and invasion assays.

Cell proliferation: Cell proliferation was performed using the CellTiter 96[®] AQueous One Solution Cell Proliferation Assay according to manufacturer's instructions (Promega). Cells were plated in 96-well plates at a density of 1000 cells per well. 10 μ l CellTiter 96[®] AQueous One Solution Reagent (Promega) was added to the cells per well, and incubated for 1 h at 37°C. Then the reaction mixture was measured in a microplate reader at 490 nm.

Cell migration and invasion assays: Cell suspension containing 1×10^5 cells/ml was added into the upper surface of the wells. The lower wells contains 20% (v/v) FBS. After 6 h migration at 37°C, the migrated cells through the inserts were fixed with 4% formaldehyde and stained by crystal violet. The invasion assay was performed by adding cells into the inside of each insert coated with Matrigel and incubating for 48 h. Then the cells that invaded to the lower surface of the wells were fixed, stained by crystal violet and counted.

In vivo xenograft tumor growth experiments

Balb/c nude mice was injected subcutaneously into the flank with 1×10^6 H1299 stable cells. Tumor sizes were measured at the indicated time. After 25 days when the tumor reached to approximately 1 cm in diameter, the tumors were dissected, and the weight of tumors were measured.

Real-time RT-PCR

Total RNA was isolated from cells using Trizol reagent (Invitrogen). Two-step real-time polymerase chain reaction (PCR) was performed using the SYBR Green dye (Roche) and a LightCycler[®] 96 detection system (Roche) according to manufacturer's instructions. Primers used were designed as follows: JMJD6 forward primer, 5'-AACTTTTGGAGACTACAAGGTGC-3'; JMJD6 reverse primer, 5'-CCCAGAGGGTTCGATGTGAATC-3'; HOXB9 forward primer, 5'-CCATTTCTGGGACGCTTAGCA-3'; HOXB9 reverse primer, 5'-TGTAAGGGTGGTAGACG GACG-3'. All mRNAs were normalized to expression of GAPDH gene found in the same sample.

Chromatin immunoprecipitation (ChIP) assay

The stable H1299 cells were crosslinked with 1% formaldehyde and subjected to chromatin immunoprecipitation (ChIP) assays as described before (27). The ChIP DNA complex were extracted and purified by DNA purification kit. Then the purified DNA was subjected to real-time RT-PCR using the specific primers listed: JMJD6 promoter 5'-GGTCACTTCTTGGCAGGGTCT-3' (forward) and 5'-TGAGGTCAGGAGCGGATGTC-3' (reverse).

Tumor tissues

The tissue specimens of lung adenocarcinomas patients were obtained from the Department of Thoracic Surgery

Sino-Japan Friendship Hospital, Beijing China (with Permit Number: ZRLW-5 and ZRLW-7). Tissue specimens were sectioned at the Department of Pathology Peking University Health Science Center, Beijing, China.

Immunohistochemical staining

Tissue sections were deparaffinized and rehydrated gradually. Antigen retrieval was performed in 10 mM sodium citrate buffer (pH 6.0) for 15 min. To quench endogenous peroxidases, the sections were incubated in 3% H₂O₂ for 30 min. After incubating with primary antibody at 4°C overnight, the PV6001 2-step plus Poly-HRP anti-rabbit IgG detection system (Zhong Shan Jin Qiao, Beijing, China) was applied. The detection was performed by streptavidin-biotin-peroxidase method. The lung cancer patient tissue sections were immunohistochemically stained by the anti-AcK27-HOXB9 specific antibody. Criteria for immunohistochemical staining were classified into four groups based on HOXB9 acetylation staining level: low staining marked as 1+, faint staining as 2+, moderate staining as 3+, and strong staining as 4+. We defined that 3+ and 4+ reactivities are high expression and the other two staining level are low expression.

Statistical analysis

Data were presented as mean \pm SEM. For a single comparison of two groups, Student's *t*-test was applied. *P* < 0.05 was considered statistically significant. Survival analyses were performed using Kaplan–Meier analysis and log-rank tests.

RESULTS

The acetyltransferase PCAF acetylates HOXB9 both *in vitro* and *in vivo*

HOXB9 was reported to function importantly in various tumors (6,12,14,29). However, there are few reports about how HOXB9 was regulated, and there was no report about the relationship between HOXB9 and post-translational modification (PTM). In an attempt to identify HOXB9 PTM, we found that HOXB9 is an acetylated protein in living cells. In detail, we firstly performed a co-immunoprecipitation with an anti-acetylated-lysine antibody in human lung adenocarcinoma H1299 cells, which were transfected with FLAG-HOXB9 expression vector. Interestingly, HOXB9 in the immunoprecipitation complex was found to be an acetylated protein (Figure 1A). Furthermore, acetylation of HOXB9 is detected after ectopic expression of acetyltransferase PCAF, but not other acetyltransferases including CBP, p300 and hMOF (Figure 1B). To exclude possible involvement of other acetylated proteins, we expressed HOXB9 and PCAF in *Escherichia coli* by fusion them with maltose-binding protein (MBP) or glutathione-S-transferase (GST) separately. We then performed *in vitro* acetylation assays using purified MBP tagged HOXB9 and GST tagged PCAF acetyltransferase catalytic HAT domain. Results showed that HOXB9 was indeed acetylated *in vitro* by PCAF, but not by the MBP tag (Figure 1C). In addition, when we performed *in vitro* acetylation assays using purified GST tagged HOXB9

and GST tagged PCAF acetyltransferase catalytic HAT domain, we found that HOXB9 was indeed acetylated *in vitro* by PCAF, but not by the GST tag (Supplementary Figure S1A). Taken together, we pinpointed for the first time that HOXB9 is able to be acetylated by PCAF, representing a paradigm that HOXB9 can be post-translationally modified.

HOXB9 interacts with PCAF both *in vitro* and *in vivo*

Given that PCAF acetylates HOXB9 we wondered that whether HOXB9 interacts with PCAF. To this end, we performed a co-immunoprecipitation assay. We found that HOXB9 was co-immunoprecipitated endogenously by PCAF in human lung adenocarcinoma H1299 and A549 cells (Figure 2A and Supplementary Figure S1B), indicating that HOXB9 interacts with PCAF in living cells. Reciprocally, PCAF was also co-immunoprecipitated by FLAG-HOXB9 in H1299 cells (Figure 2B). Furthermore, exogenously expressed HOXB9 and PCAF were able to be co-immunoprecipitated by each other using different tag antibodies (Figure 2C and D). These results clearly indicated that there is an interaction between HOXB9 and PCAF both endogenously and exogenously in living cells. To determine the binding regions between HOXB9 and PCAF, we first constructed and expressed three GST-fusion proteins from *E. coli* that contain HOXB9 full-length (1–250), the N-terminal (1–184) and homeobox (185–250) domains separately. GST pull-down assays showed that PCAF mainly interacts with the full-length protein and the N-terminal domain of HOXB9, although there existed a weak interaction between PCAF and the homeobox domain of HOXB9 (Figure 2E). We then constructed and expressed four GST-fusion proteins from *E. coli* that contain the N-terminal, HAT, ADA and BROMO domains of PCAF. The following GST pull-down assay showed that HOXB9 interacts with the N-terminal, HAT and ADA domains of PCAF but not the BROMO domain (Figure 2F). Furthermore, immunofluorescence staining showed that HOXB9 and PCAF are able to colocalize in the nucleus (Figure 2G). Thereby, these data demonstrated that HOXB9 interacts with PCAF both *in vitro* and *in vivo*.

HOXB9 is acetylated at residue K27 by PCAF

Given that PCAF interacts with and acetylates HOXB9 both *in vivo* and *in vitro*, we therefore wanted to identify the acetylation sites of HOXB9. To this end, we co-transfected FLAG-HOXB9 with FLAG-PCAF expression vectors, followed by co-immunoprecipitation. Then we performed SDS-PAGE, the bands containing FLAG-HOXB9 were taken out and analyzed by LC-MS/MS. Interestingly, we found that five lysines (K27, K117, K159, K167 and K202) of HOXB9 were acetylated in the cells (Figure 3A). Next, we replaced the five acetylated lysines with arginines by mutagenesis and generated five mutants with change of K to R (mimics of acetylation-deficient HOXB9). We then co-transfected different HOXB9 mutants with FLAG-PCAF into the HEK-293T cells and found that only mutant K27R significantly reduced the acetylation level of HOXB9 compared to that of the wild type (WT) HOXB9 (Figure

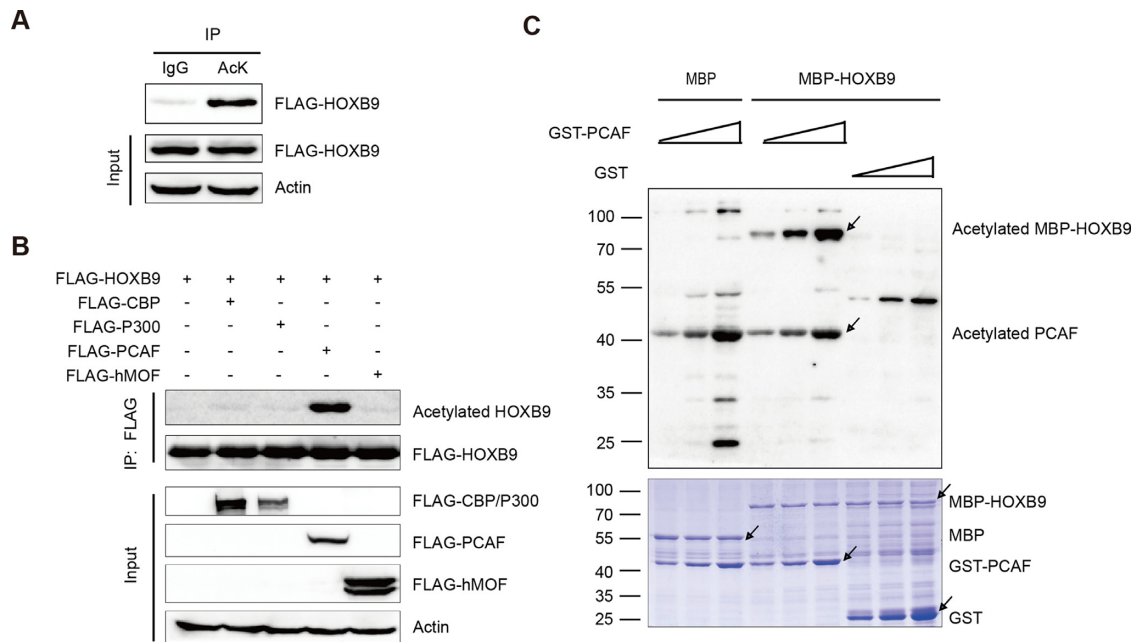


Figure 1. HOXB9 is acetylated by PCAF in cells. (A) HOXB9 is acetylated in H1299 cells. H1299 cells transfected with FLAG-HOXB9 expression vector and were treated with 3 μ M TSA and 5 mM nicotinamide for 12 h, and then cell lysates were immunoprecipitated with an anti-acetylated-lysine (AcK) antibody or normal IgG, followed by immunoblotting with an anti-FLAG antibody. (B) PCAF acetylated HOXB9 *in vivo*. FLAG-HOXB9 expression vector was cotransfected separately with expression vectors containing a variety of acetyltransferases into H1299 cells. Forty-eight hours post transfection, cell lysates were immunoprecipitated with an anti-FLAG antibody, followed by Western blot analysis with the AcK antibody. (C) PCAF acetylated HOXB9 *in vitro*. The *in vitro* acetylation assays were performed by using MBP, MBP-fusion proteins of HOXB9, and various amounts GST-fusion PCAF HAT domain. Then the reaction mixtures were subjected to SDS-PAGE, and followed by immunoblotting with the AcK Ab. The purified MBP and GST tagged fusion proteins were stained by Coomassie blue. Arrows showed the correct molecular masses of the indicated proteins.

3B), suggesting that K27 is the major acetylation site of HOXB9 by PCAF.

To examine whether K27 of HOXB9 can be acetylated *in vivo*, we generated a rabbit polyclonal antibody that is specific to the acetylated K27. The specificity of the AcK27-HOXB9 antibody was verified by its ability to recognize the acetylated, but not unacetylated HOXB9 peptides (Figure 3C). Furthermore, the AcK27-HOXB9 antibody recognized ectopically expressed WT-HOXB9, but not the K27R acetylation-deficient mutant (Figure 3D). In a clean *in vitro* system, purified MBP- tagged HOXB9-WT and K27R mutants were used for *in vitro* acetylation assays which were mixed with GST-PCAF-HAT. Convincingly, the AcK27-HOXB9 antibody was found to recognize WT-HOXB9 only, but not the K27R mutant (Figure 3E). These data strongly demonstrated that the AcK27-HOXB9 antibody is specific for the recognition of HOXB9 acetylation at K27 both *in vivo* and *in vitro*. Next, in order to investigate the conservation of HOXB9-K27 among other species during evolution, we compared the amino acid sequence of HOXB9 aligned with other seven species. Interestingly, we found that HOXB9-K27 is highly conserved in multiple species (Figure 3F), suggesting that HOXB9-K27 in other species might be acetylated by PCAF as well. Moreover, when we knocked down endogenous PCAF with small interfering RNA (siRNA) in H1299 cells, we found that the acetylation level of HOXB9 in PCAF depleted cells was decreased compared to the control cells, indicating that PCAF is indeed responsible for HOXB9 acetylation (Figure 3G). Moreover, the immunohistochemical staining by AcK27-

HOXB9 antibody in mouse tissues indicated that HOXB9 acetylation existed in multiple mouse tissues including lung, brain, kidney, uterus and ovary, but not in lymph node (Figure 3H and Supplementary Figure S2), suggesting that HOXB9 acetylation may function physiologically. Collectively, these findings demonstrated that K27 is the major acetylation site of HOXB9 and is conserved during the evolution.

SIRT1 deacetylates and interacts with HOXB9

It was known that the protein acetylation and deacetylation are a balanced process. In order to identify the deacetylases that are responsible for HOXB9 deacetylation, we applied TSA, the class I and II histone deacetylase (HDAC) inhibitor, and nicotinamide, the class III sirtuin (SIRT) inhibitor. Treatment of cells with SIRT inhibitor nicotinamide, but not HDAC inhibitor TSA, the HOXB9 acetylation level was found significantly raised (Figure 4A). This suggested that SIRT family members may be preferentially involved in HOXB9 deacetylation. Then we co-expressed HOXB9 with HDAC members including HDAC1, HDAC2, HDAC3 and SIRT members including SIRT1 and SIRT2 deacetylases in H1299 cells. Interestingly, we found that only SIRT1, but not other deacetylases remarkably decreased HOXB9 acetylation (Figure 4B). Furthermore, nicotinamide was found to be able to reverse HOXB9 acetylation under SIRT1 overexpression (Figure 4C). In contrast, the acetylation level of HOXB9 was drastically increased when endogenous SIRT1 was knocked down with SIRT1

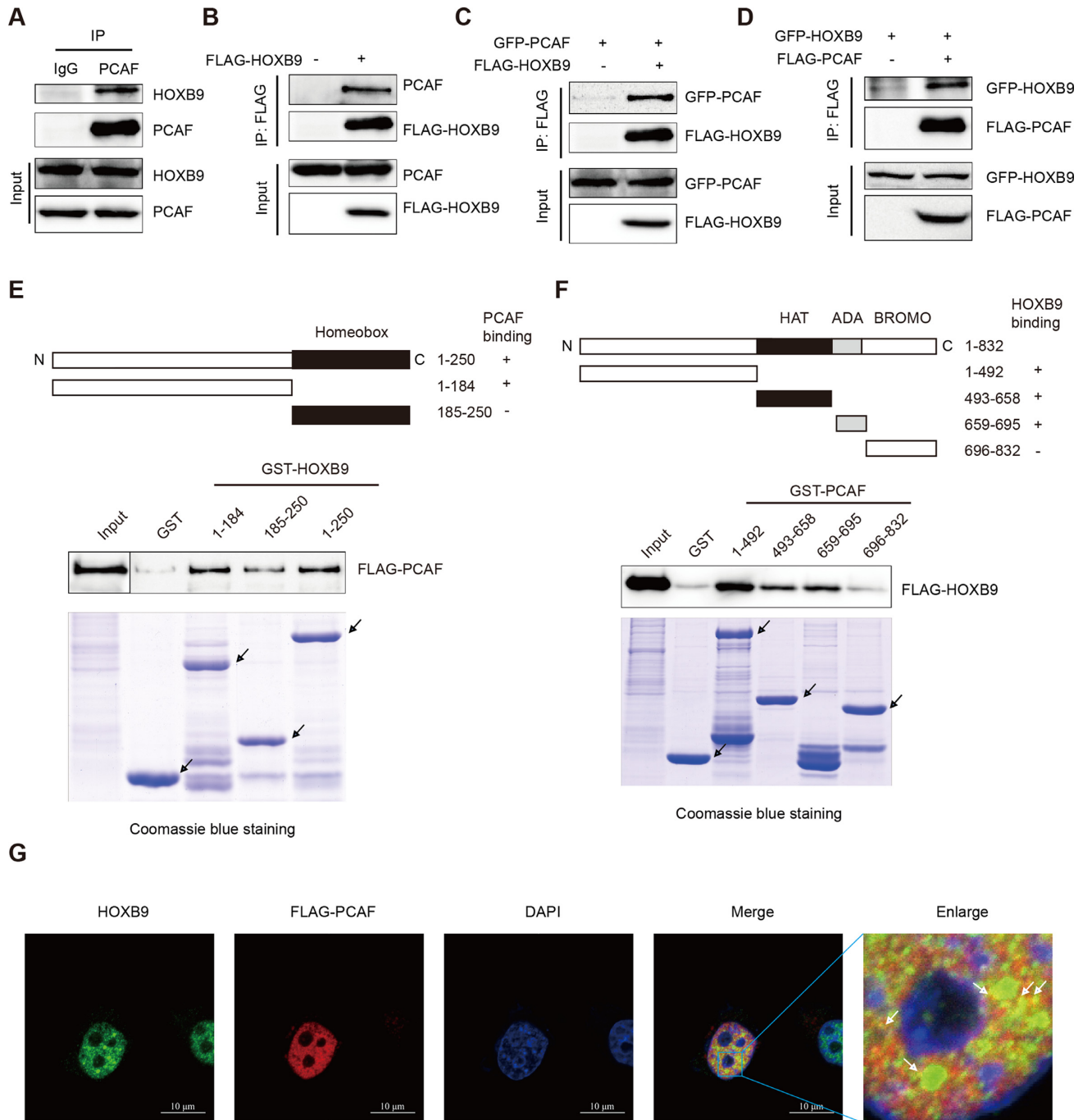


Figure 2. HOXB9 interacts with PCAF both *in vivo* and *in vitro*. (A–D) HOXB9 interacts with PCAF *in vivo*. Co-immunoprecipitation assays were performed using lysates from H1299 cells with control IgG or anti-PCAF antibody, followed by immunoblotting with an anti-HOXB9 antibody (A). HEK-293T cells were transfected with FLAG-HOXB9 expression vector. Lysates were co-immunoprecipitated by an anti-FLAG antibody, followed by immunoblotting with an anti-PCAF antibody (B). GFP-PCAF and FLAG-HOXB9 expression vectors were co-transfected into HEK-293T cells, immunoprecipitated with a FLAG antibody, and detected with indicated antibodies (C). HEK-293T cells were transfected with FLAG-PCAF and GFP-HOXB9 expression vectors, immunoprecipitated with FLAG antibody, followed by immunoblotting with indicated antibodies (D). (E) Upper panel: A schematic diagram of HOXB9 domains. Bottom panels: GST pull-down assays were performed using HEK-293T cell lysates transfected with FLAG-PCAF expression vector. Different GST tagged proteins were purified and incubated with cell lysates. Glutathione beads were added into the complex, and the bound mixture was subjected to SDS-PAGE, followed by immunoblotting with an anti-FLAG antibody. The purified GST-HOXB9 fusion proteins were shown by Coomassie blue staining. Arrows indicated the correct molecular masses of corresponding proteins. (F) Upper panel: A schematic diagram of PCAF domains. Bottom panels: HEK-293T cell lysates transfected with FLAG-HOXB9 expression vector were used in GST pull-down assays. The pulled down protein mixture was subjected to SDS-PAGE, followed by immunoblotting with an anti-FLAG antibody. The purified GST-PCAF fusion proteins were detected by Coomassie blue staining. Arrows indicated the correct molecular masses of corresponding proteins. (G) HOXB9 colocalized with PCAF in cell nuclei. H1299 cells were transfected with FLAG-PCAF expression vector, and stained with an anti-HOXB9 mab (green) and an anti-FLAG pab (red). Nuclei were stained with DAPI (blue), followed by visualization with confocal microscopy. Scale bars: 10 μ m. Arrows showed the colocalized region.

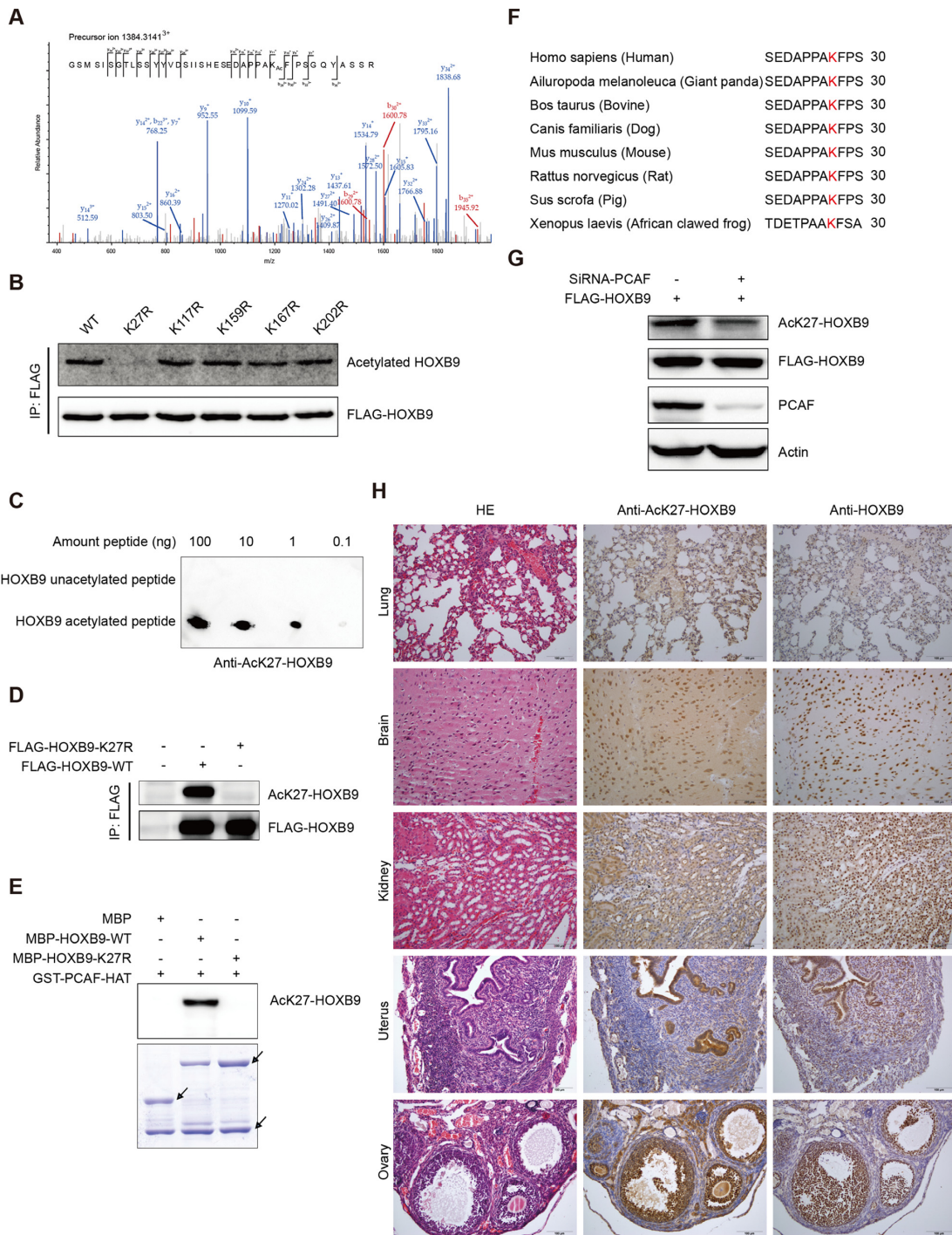


Figure 3. HOXB9 is identified to be acetylated at lysine 27. (A) The spectrum of the charged ion (m/z 1384.3141) indicated that lysine 27 is acetylated (lower case Ac) in the peptide GSMSISGLTSSYYVDSIISHSEDAAPPKFPSPGQYASSR. The b ions indicate the fragmentation ions containing the N-terminus of the peptide and the y ions are the fragmentation ions containing the C-terminus of the peptide. (B) Mutation of K27 significantly decreases HOXB9 acetylation. HEK-293T cells were co-transfected with different FLAG tagged HOXB9 mutants and PCAF. Cell lysates were co-immunoprecipitated with anti-FLAG antibody, immunoblotted with the AcK antibody. (C) Specificity of antibody against AcK27-HOXB9 was verified by dot blot assays. Nitrocellulose membrane was spotted by different amounts of HOXB9 unacetylated peptide (EDAPPAKFPSPGQYAC), HOXB9 acetylated peptide (EDAPPA(AcK)FPSPGQYAC), and detected with the anti-AcK27-HOXB9 antibody. (D) HOXB9-WT and HOXB9-K27R mutant expression vectors were co-transfected into HEK-293T cells, then subjected to SDS-PAGE, followed by immunoblotting with the anti-AcK27-HOXB9 antibody. (E) *In vitro* acetylation assays were performed using GST-PCAF HAT domain and different purified mutants of MBP-HOXB9. The reaction mixtures were subjected to SDS-PAGE, immunoblotted with the anti-AcK27-HOXB9 specific antibody. (F) The sequences adjacent to human HOXB9-K27 from different HOXB9 homologues species were aligned. (G) H1299 cells were transfected with FLAG-HOXB9. Endogenous PCAF was knocked down with small interfering RNA (siRNA). Cell lysates were subjected with SDS-PAGE, followed by immunoblotting with the indicated antibodies. (H) A variety of tissues from C57BL6 mouse were performed by immunohistochemical staining with anti-AcK27-HOXB9 and anti-HOXB9 total antibodies respectively.

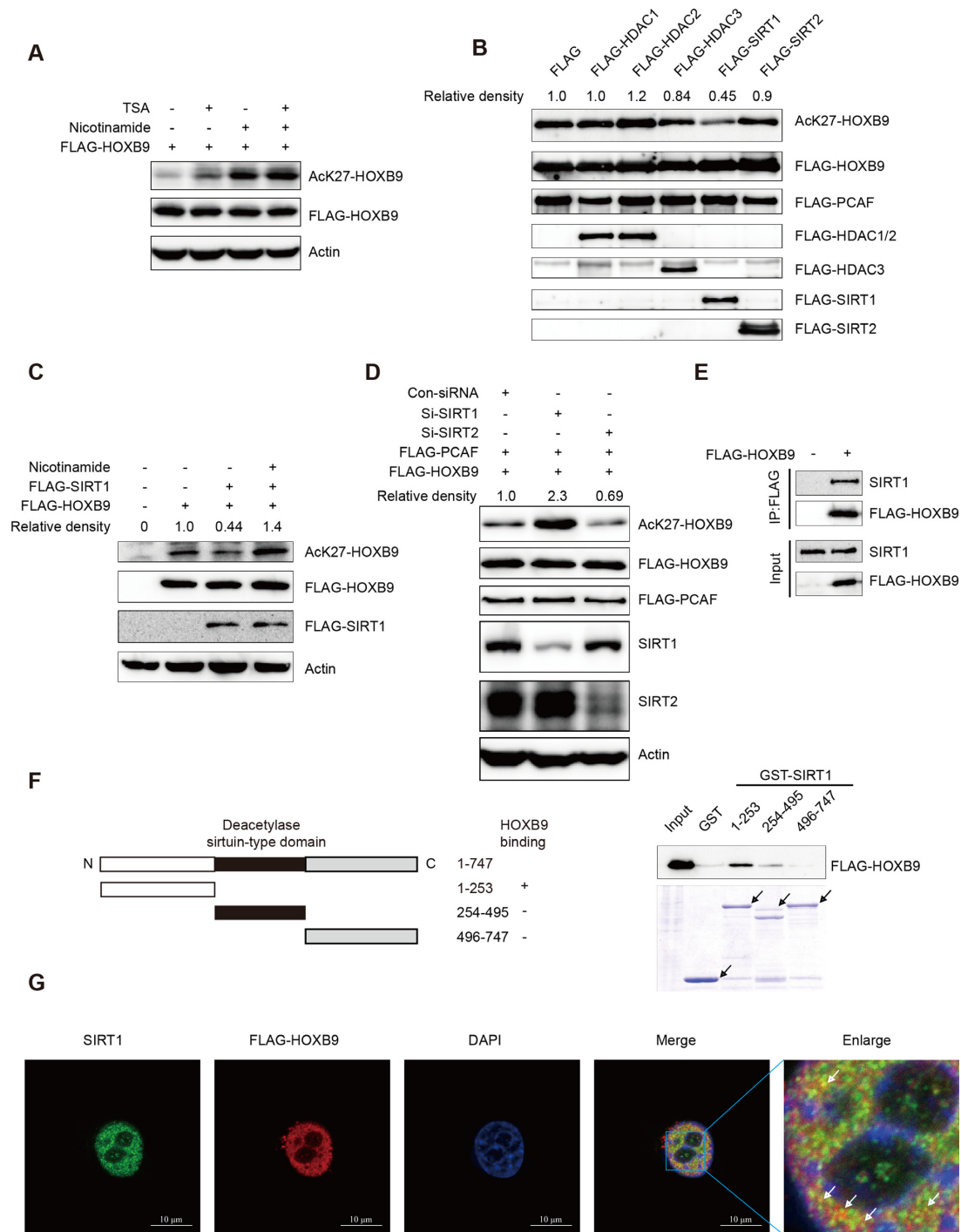


Figure 4. HOXB9 is deacetylated by SIRT1 *in vivo* and *in vitro*. (A) SIRT inhibitor nicotinamide increased HOXB9 acetylation level. H1299 cells were transfected with FLAG-HOXB9 expression vector, and treated with 3 μ M TSA or 5 mM nicotinamide for 12 h. Cell lysates were subjected to SDS-PAGE, followed by immunoblotting with the anti-AcK27-HOXB9 antibody. (B–D) SIRT1 deacetylated HOXB9. H1299 cells were co-transfected separately with expression vectors containing FLAG tagged HOXB9, PCAF and different deacetyltransferases. Western blot analysis was performed with the indicated antibodies (B). H1299 cells were co-transfected with FLAG-HOXB9 and FLAG-SIRT1 expression vectors, then treated with 5 mM nicotinamide for 12 h, Western blot analysis was performed with the indicated antibodies (C). H1299 cells were co-transfected with FLAG-HOXB9 and FLAG-PCAF expression vectors together with small interfering RNA (siRNA) against SIRT1 or SIRT2. Cell lysates were subjected to Western blot analysis using the anti-AcK27-HOXB9 antibody (D). (E and F) HOXB9 interacts with SIRT1 *in vivo*. H1299 cells were transfected with FLAG-HOXB9 expression vector. The cell lysates were co-immunoprecipitated with anti-FLAG antibody, followed by Western blot analysis with the indicated antibodies (E). Left panel: A schematic diagram of SIRT1 domains. Right panels: HEK-293T cells were transfected with FLAG-HOXB9 expression vector. The cell lysates were incubated with different GST-fusion domains of SIRT1 respectively. GST pull-down mixture was subjected to Western blot analysis with an anti-FLAG antibody. Arrows indicate the correct molecular masses (F). (G) HOXB9 was colocalized with SIRT1. H1299 cells were transfected with FLAG-HOXB9 expression vector. Then anti-SIRT1 (green) and anti-FLAG (red) antibodies were applied for immunofluorescent staining. Nuclei were stained with DAPI (blue), and were visualized by confocal microscopy. Scale bars: 10 μ m. Arrows showed the colocalized region.

small interfering RNA (siRNA), but not SIRT2 siRNA (Figure 4D). These data clearly indicated that HOXB9-K27 acetylation is deacetylated by SIRT1. To examine whether SIRT1 interacts with HOXB9 we performed a co-immunoprecipitation assay. Interestingly, SIRT1 was found to be co-immunoprecipitated by HOXB9 in human lung adenocarcinoma H1299 and A549 cells (Figure 4E and Supplementary Figure S1C). To map which domain of SIRT1 binds to HOXB9, we constructed and purified three GST tagged SIRT1 from *E. coli* (Figure 4F left). The following GST pull-down assay showed that HOXB9 interacts with mainly the N-terminal (1–253) domain of SIRT1, but not other domains (Figure 4F right). In addition, HOXB9 and SIRT1 were also found to be colocalized in the nucleus (Figure 4G). Therefore, we pinpointed out that SIRT1 is a HOXB9-interacting protein that deacetylates HOXB9, suggesting that the acetylation of HOXB9 is a dynamic and tightly regulated process in living cells.

Acetylation of HOXB9 suppresses lung cancer cell migration and xenografted tumor growth

To further explore the physiological function of HOXB9 acetylation, we investigated the effect of HOXB9-K27 acetylation on lung cancer cell migration and tumor growth in mice. We first established H1299 cells stably expressing FLAG tagged HOXB9-WT, HOXB9-K27R and HOXB9-K27Q (a mimic of hyperacetylated HOXB9) separately (Figure 5A). Consistent with the previous report (13), overexpressed HOXB9-WT caused a significant increase of H1299 cell migration and invasion. Cells expressing HOXB9-K27R notably promoted lung cancer cell migration and invasion compared to the HOXB9-WT, whereas expression of HOXB9-K27Q decreased these abilities compared to the HOXB9-WT (Figure 5B and C). To examine the role of HOXB9 acetylation in tumor growth, we performed mouse xenograft assays using the H1299 stable cell lines expressing HOXB9-WT, HOXB9-K27R or HOXB9-K27Q. As shown in Figure 5D–F, cells expressing acetylation-deficient mutant HOXB9-K27R displayed a faster tumor growth rate and larger tumor volumes than that of the HOXB9-WT. However, cells expressing the hyperacetylated mutant HOXB9-K27Q displayed a slower tumor growth rate and smaller tumor volumes than that of the HOXB9-WT. Taken together, these results strongly suggested that acetylation at K27 of HOXB9 suppresses lung cancer cell migration and tumor growth in mice.

Acetylation-deficient HOXB9-K27 mutant promotes JMJD6 transcription

To uncover the molecular mechanism underlying acetylated HOXB9 regulation on cell migration and tumor growth, we examined the gene expression profiles using H1299 stable cells expressing HOXB9-K27R, HOXB9-WT or empty vector. The genes from microarray analyses that change in HOXB9-WT when compared to Vector, are thought to be regulated by HOXB9, and the genes that change in HOXB9-K27R when compared to HOXB9-WT, are thought to be regulated by HOXB9 acetylation (Figure 6B). Therefore, the 729 overlapping genes (fold >1.5) we se-

lected from the microarray analyses are thought to be regulated by both HOXB9 and its acetylation (Figure 6A). We have performed the KEGG enrichment analysis in the 729 overlapping genes. We found that HOXB9 acetylation was involved in many pathways, including PPAR signaling pathway, Calcium signaling pathway, Cell adhesion molecules (CAMs) and Glycosaminoglycan biosynthesis-heparan sulfate/heparin, etc. (Supplementary Figure S3A). We thus reasoned the genes that are transcriptionally activated (155 genes) or downregulated (53 genes) in the combo of HOXB9-K27R, HOXB9-WT and empty vector are likely targets of HOXB9-K27 acetylation (Figure 6B). Among the 208 upregulated or downregulated overlapping genes, JMJD6 was noted to act as a histone arginine demethylase and a lysyl-hydroxylase (30,31). JMJD6 has been reported upregulated in multiple cancers, including lung adenocarcinoma, breast ductal carcinoma, and colon adenocarcinoma (31–33). We thus selected JMJD6 as an example to scrutinize the transcriptional mechanism of HOXB9 acetylation. To this end, we performed a real-time RT-PCR to validate the microarray data. Consistently, we found that the expression of JMJD6 was upregulated by HOXB9, and the expression level was increased further by the presence of HOXB9-K27 acetylation-deficient mutant (Figure 6C). Western blot analysis also demonstrated that JMJD6 was upregulated by the expression of HOXB9-K27R mutant compared to that of the wild type HOXB9 (Figure 6D). In addition, we analyzed the correlation of HOXB9 and JMJD6 expression in 40 lung adenocarcinomas patient samples in GEO datasets and found a positive correlation between HOXB9 and JMJD6 mRNA expression levels (GDS3627, $R = 0.4554$, $P = 0.0032$) (Figure 6E). To investigate whether JMJD6 is a direct target gene of HOXB9, we performed ChIP assays. ChIP results showed that HOXB9 binds to the promoter of JMJD6. Furthermore, HOXB9 acetylation-deficient mutant K27R displayed an enhanced binding ability to the JMJD6 promoter compared to that of the wild type (Figure 6F). In contrast, HOXB9-WT and K27R mutant was not found at the promoter of the Actb gene. Thus, the Actb gene was used as a negative control indicating that the ChIP assay is site-specific (Figure 6F). These data suggested that JMJD6 is a direct target of HOXB9. Functionally, we found that HOXB9 acetylation-deficient mutant K27R showed a stronger ability in promoting H1299 cell growth compared to that of the wild type (Figure 6H). Under the depletion of JMJD6 by RNAi, JMJD6 was found to be required for H1299 cell growth promoted by HOXB9 acetylation-deficient mutant K27R (Figure 6G and H). In addition, HOXB9 affects not only the transcription of JMJD6, but also other oncogenic proteins, including MMP1 and ZEB2 included in our microarray data, which were also validated by real-time RT-PCR (Supplementary Figure S3B). Therefore, JMJD6 is an important downstream effector that mediates HOXB9 and acetylated HOXB9 regulated lung cancer progression.

Elevated K27 acetylation of HOXB9 predicts a favorable survival in lung adenocarcinoma patients

Given that the acetylation-deficient HOXB9-K27 mutant promotes lung cancer cell migration and tumor growth

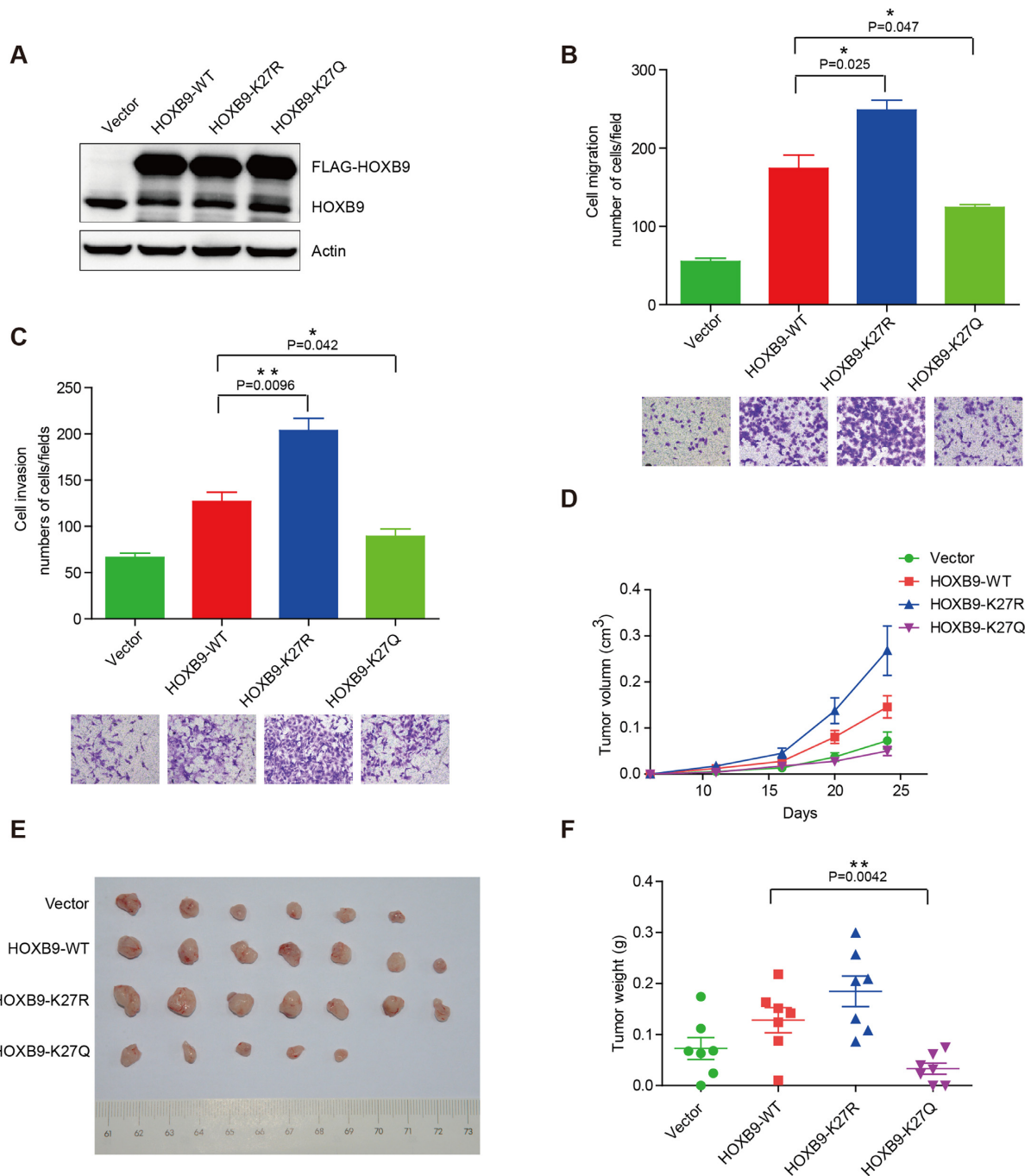


Figure 5. HOXB9 acetylation inhibits lung cancer cell migration and tumor growth. (A) The H1299 cells stably expressed HOXB9-WT, HOXB9-K27R and HOXB9-K27Q were established and the expression of target proteins was verified by western blot analysis using HOXB9 antibody. (B) The effect of HOXB9 acetylation on H1299 cell migration was determined. Data were presented as mean \pm SEM from three independent experiments. The statistical analyses were performed by Student's *t*-test, * for $P < 0.05$. Representative images of the stable H1299 cell migration were shown at the bottom panel. (C) The effect of HOXB9 acetylation on H1299 cell invasion was assayed. Data were presented as mean \pm SEM from three independent experiments. The statistical analyses were performed by Student's *t*-test, * for $P < 0.05$, ** for $P < 0.01$. Representative images of stable H1299 cell invasion on Matrigel were shown at the bottom panel. (D–F) Unacetylated HOXB9 promotes tumor growth in nude mice. Mice were injected with stable H1299 cells and the control cells. Tumor growths in xenografted nude mice were measured and plotted (D). The xenograft tumors were dissected and photographed at day 25 (E). Average tumor weights were measured at day 25 (F), the statistical analyses were performed by Student's *t*-test, ** for $P < 0.01$.

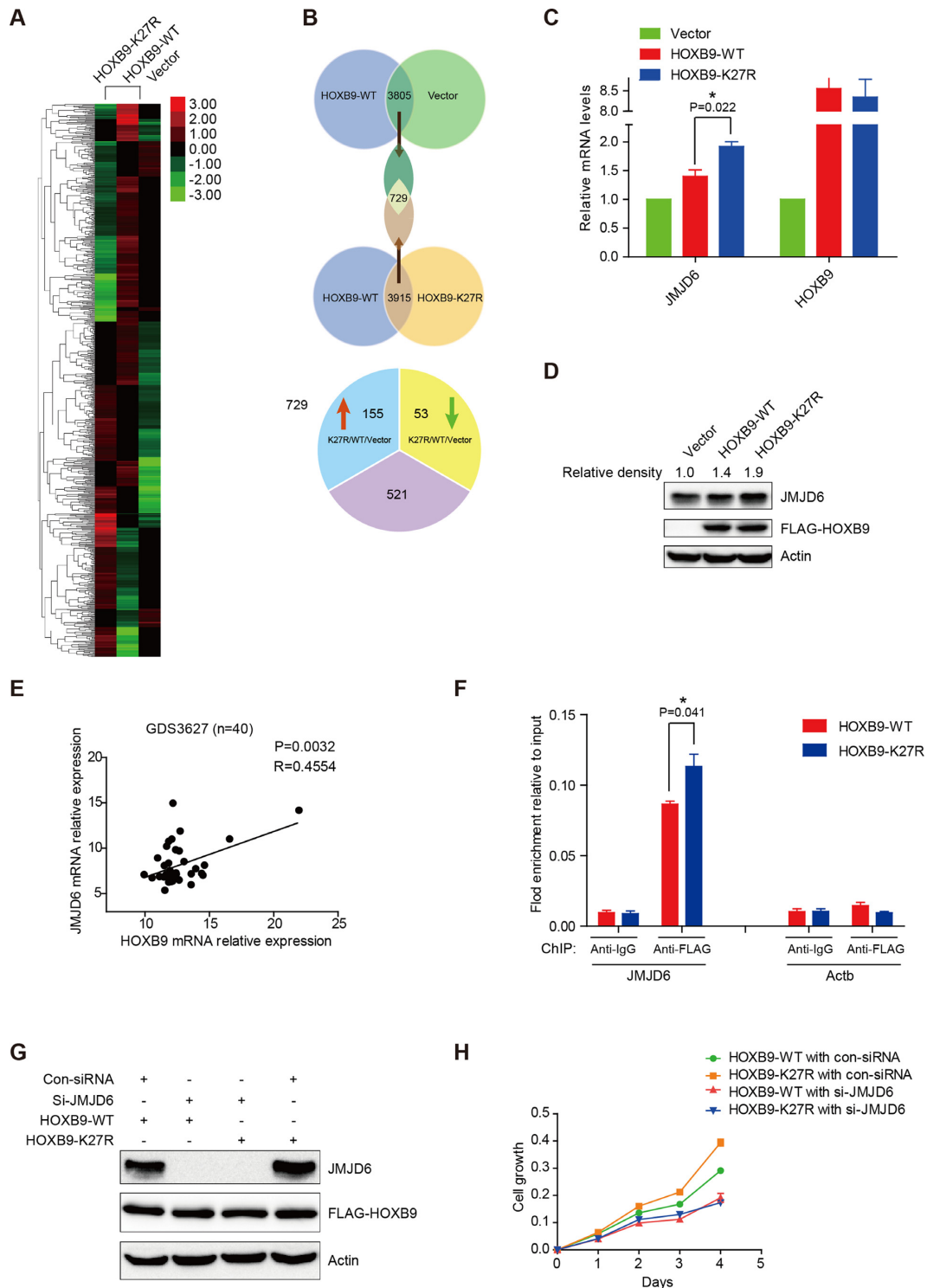


Figure 6. Acetylation-deficient HOXB9-K27R mutant promotes JMJD6 gene transcription. (A) The heatmap of 729 overlapping genes that exhibited expression differences between HOXB9-K27R, WT and vector. (B) The crosstalk of gene expression profiling analysis was shown to identify target genes regulated by HOXB9 and its acetylation. (C) Real-time RT-PCR analysis of JMJD6 and HOXB9 gene expressions in H1299 cells stably expressing HOXB9-WT and HOXB9-K27R, controlled by empty vector. Data were presented as mean \pm SEM from three independent experiments. The statistical analyses were performed by Student's *t*-test, * for $P < 0.05$. (D) JMJD6 levels in H1299 cells stably expressing HOXB9-WT, HOXB9-K27R or control were analyzed by Western blot analysis using JMJD6 antibody. (E) Analysis of the correlation between HOXB9 and JMJD6 gene expression of 40 lung adenocarcinomas patient samples in GEO datasets. (F) ChIP assays were performed using control IgG or an anti-FLAG Ab in H1299 cells. The binding of HOXB9 on promoters of JMJD6 and the negative control Actb were analyzed by qPCR. Data were presented as mean \pm SEM from three independent experiments. The statistical analyses were performed by Student's *t*-test, * for $P < 0.05$. (G) H1299 stable cells with JMJD6 knocked down were analyzed by western blot analysis using a JMJD6 antibody. (H) Cell proliferation assays were performed when JMJD6 was knocked down in H1299 cells stably expressing HOXB9-WT and HOXB9-K27R mutant.

in mice as shown above it is tempting to know whether HOXB9-K27 acetylation exists differentially in lung adenocarcinoma patients. To this end, we examined the levels of HOXB9-K27 acetylation in a cohort of 75 lung adenocarcinoma patients analyzed by immunohistochemistry using the anti-AcK27-HOXB9 specific antibody. Interestingly, we found that the level of HOXB9 acetylation correlated significantly with the outcome of lung adenocarcinoma patients, and the patients with elevated HOXB9 K27 acetylation had a better overall survival than those who displayed lower acetylation of HOXB9-K27 (Figure 7A). Further, higher level of HOXB9 acetylation correlated significantly with smaller tumor size, less lymph node metastasis and AJCC category (Figure 7B–D). In the same cohort of lung adenocarcinoma patients, we also examined the protein levels of JMJD6. Consistent with the previous reports (32), the protein level of JMJD6 was higher in lung adenocarcinomas than the normal lung tissues (Figure 7E and F), and patients with elevated JMJD6 levels had a poor overall survival (Figure 7G), supporting that JMJD6 indeed acts as an oncogenic protein. Given that JMJD6 is a target gene for HOXB9 acetylation, we then examined the correlation between acetylated HOXB9 and JMJD6 in lung adenocarcinoma patients. As a paradigm, a negative correlation between acetylated HOXB9 and JMJD6 was indeed identified in representative images of patient samples stained by immunohistochemistry using the anti-AcK27-HOXB9 specific antibody and JMJD6 antibody (Figure 7H and I). Collectively, these findings firmly suggested that HOXB9 acetylation level may be of prognostic value for lung adenocarcinoma patients, in which elevated HOXB9 acetylation may predict a favorable outcome for the patients.

DISCUSSION

In this study, we provided evidence that homeobox superfamily member HOXB9 is an acetylated protein, for the first time demonstrating that HOXB9 is able to be post-translationally modified. Moreover, we identified that acetyltransferase PCAF acetylates and interacts with HOXB9 both *in vitro* and *in vivo*. Acetylation is a dynamic process and can be reversed by specific deacetylases, we then continued to pinpoint that SIRT1 is the deacetylase that deacetylates HOXB9. Furthermore, using LC-MS/MS and mutation techniques, we showed that K27 is the main acetylation site of HOXB9, a site that is able to be acetylated in multiple normal tissues and tumors.

HOXB9 was reported to play different roles in cancer progression. It was known that HOXB9 functions as a tumor promoting gene in lung and breast cancers (11,13). However, it was also found that HOXB9 plays a tumor suppressive role in colon, gastric and pancreatic cancers (14,16,17). The diverse roles of HOXB9 in different cancer types suggest that the functions of HOXB9 are complex. For example, the acetylation at K27 of HOXB9 inhibited the function of HOXB9 in promoting lung cancer cell migration and tumor growth as we reported here. These findings hinted that the differential post-translational modifications (PTMs) of HOXB9 may be involved in specific biological functions. The dynamic balance of HOXB9 acetylation and deacetylation seems to indicate that HOXB9 acetyla-

tion is tightly regulated. Thereby the acetylation of HOXB9 may represent an important mode underlying HOXB9 precise control of target gene expression in physiological and pathological processes. In addition, we also observed that the acetylation level of HOXB9 have no correlation with HOXB9 protein stability (data not shown). To elucidate the reason why HOXB9 acetylation attenuates its function, we performed a microarray-based gene expression analysis and found that there are 729 overlapping genes (fold > 1.5) that are coregulated by HOXB9 and acetylated HOXB9. It is very important to identify the target genes of HOXB9 and acetylated HOXB9 because HOXB9 is known to play different roles in tumor progression, but the mechanism is still unclear until now.

The microarray gene expression profiling analyses indicated that the Jumonji domain-containing 6 (JMJD6) was coregulated by HOXB9 and HOXB9-K27 acetylation mutant. JMJD6 was found to be upregulated by HOXB9, and was further increased by HOXB9-K27 acetylation mutant. JMJD6 belongs to the family of the Jumonji C domain-containing proteins, which have been characterized as histone demethylases (34). JMJD6 was reported to function in lysyl hydroxylation, RNA splicing, and chromatin remodeling (30,35–38). However, there were conflicting reports about this function of JMJD6 in catalysing N-methyl-arginine residue demethylation on the N-terminus of the human histones H3 and H4. The direct role of JMJD6 in N-methyl-arginine demethylation was not clearly validated, because of the selectivity of the antibodies used in living cells has not been fully defined (39). Moreover, JMJD6 was found to be involved in multiple cancers including lung adenocarcinoma, breast ductal carcinoma, and colon adenocarcinoma (31–33). JMJD6 catalyzes the hydroxylation of p53 to regulate colon cancer progression (31). Recently, JMJD6 was reported to regulate Aire expression, which is critical for the establishment of immunological self-tolerance in the thymus (40). However, how JMJD6 is regulated remains elusive. In support of our findings we analyzed the GEO datasets and identified a positive correlation between HOXB9 and JMJD6 expression. In ChIP assays we pointed out that JMJD6 is an important downstream target of HOXB9 by showing that HOXB9 binds directly to the promoter of JMJD6. Intriguingly, acetylation deficient mutant K27R enhanced the HOXB9 binding ability compared to the wild type HOXB9 (Figure 6). Direct targeting to JMJD6 transcription well explained the mechanism accounting for the suppression of lung cancer cell migration and tumor growth by HOXB9 acetylation at K27. However, it is also necessary to search for other HOXB9 acetylation target genes except JMJD6 to answer the diverse roles of HOXB9 in embryonic development and cancers in future investigations.

Lung adenocarcinoma is the most common cancer type and is the leading cause of cancer death during recent decades (41,42). Many studies have indicated that some pathological parameters, such as tumor-positive lymph nodes and tumor size are of prognostic value for lung adenocarcinoma patients (43). However, there are no reliable factors that predict the progression of lung adenocarcinoma. Previous report had demonstrated that HOXB9 is upregulated in lung adenocarcinomas but not in the normal

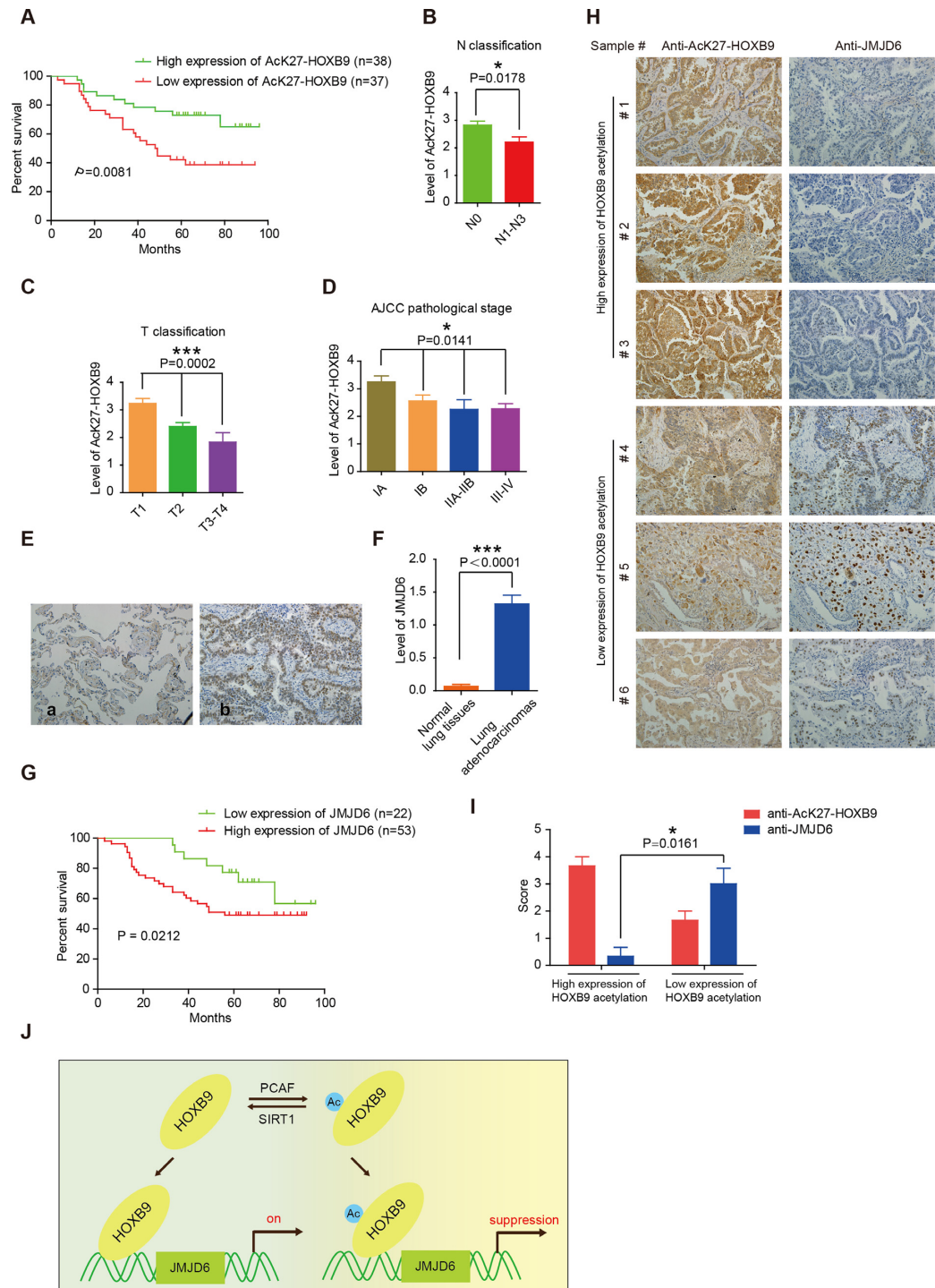


Figure 7. Elevated HOXB9-K27 acetylation is associated with longer overall survival in lung adenocarcinoma patients. (A) Immunohistochemical analysis for lung adenocarcinoma was performed using the anti-AcK27-HOXB9 antibody, and Kaplan–Meier analysis was performed in two groups of lung adenocarcinoma patients with strong staining (3+ and 4+) and weak staining (1+ and 2+) for HOXB9-K27 acetylation, with a log-rank at $P = 0.0081$. (B–D) The protein level of HOXB9-K27 were analyzed based on TNM classification (B–C) and AJCC category (D), the statistical analyses were performed by Student’s t-test (B) and one way ANOVA analyses (C–D), * for $P < 0.05$, *** for $P < 0.001$. (E) Representative images of JMJD6 in normal lung tissue (a) and lung adenocarcinoma (b). (F) The expression level of JMJD6 was analyzed in normal lung tissue and lung adenocarcinoma. The statistical analyses were performed by Student’s t-test, *** for $P < 0.001$. (G) Kaplan–Meier analysis was performed in two groups of lung adenocarcinoma patients with strong staining and weak staining of JMJD6 separately (log-rank of $P = 0.0212$). (H) Representative images of immunohistochemical staining with AcK27-HOXB9 and JMJD6 antibodies separately in six lung adenocarcinoma patients. (I) Analyses of the expression level of AcK27-HOXB9 and JMJD6 in the two group (higher and lower expression). The statistical analyses were performed by Student’s t-test, * for $P < 0.05$. (J) A working model depicts how HOXB9 is regulated by acetylation. In this model, we demonstrated that HOXB9 is acetylated by acetyltransferase PCAF, and deacetylated by deacetylase SIRT1. Acetylation of HOXB9 decreased its capacity in promoting lung cancer cell migration and tumor growth in mice by suppressing the transcription of its target gene Jumonji domain-containing protein 6 (JMJD6).

lung tissues (13). For clinical relevance, we found that the lung adenocarcinoma patients expressing elevated HOXB9-K27 acetylation had a better overall survival. Moreover, higher HOXB9 acetylation level obviously correlated with smaller tumor size and less lymph node metastasis, suggesting that the status of HOXB9-K27 acetylation is involved in the regulation of tumor progression. For the interrelationship of HOXB9-K27 acetylation with JMJD6 in lung adenocarcinomas, we identified a reciprocal correlation for the two by demonstrating that the expression of JMJD6 is higher and the level of HOXB9-K27 acetylation is lower in the representative patients (Figure 7). Therefore, these results indicated that the status of HOXB9 acetylation is of prognostic value for lung adenocarcinoma patients.

In summary, in the present investigation we identified the first PTM of homeobox transcriptional factor HOXB9. We demonstrated that HOXB9 is acetylated by PCAF at K27 and is deacetylated by SIRT1. High acetylation of HOXB9 in lung adenocarcinomas correlates with a favorable outcome for the patients. However, the generic role of HOXB9 acetylation *in vivo* might be investigated using models such as HOXB9-K27R (or Q) knock-in and HOXB9-K27R (or Q) transgenic mice in the future works. Whether there are any other PTMs including phosphorylation, methylation or ubiquitination except acetylation in HOXB9 protein remains an open question. It is tempting to uncover the mutual modulations between HOXB9 acetylation and other possible PTMs.

SUPPLEMENTARY DATA

Supplementary Data are available at NAR Online.

ACKNOWLEDGEMENTS

Ministry of Science and Technology of China [2015CB553906, 2013CB910501, 2013ZX09401-004-006]; National Natural Science Foundation of China [81230051, 81472734, 31170711, 81321003, 30830048]; Beijing Natural Science Foundation [7120002]; 111 Project of the Ministry of Education, Peking University [BMU20120314, BMU20130364]; Leading Academic Discipline Project of Beijing Education Bureau (to H.Z.). Funding for open access charge: Ministry of Science and Technology of China [2015CB553906, 2013CB910501, 2013ZX09401-004-006]; National Natural Science Foundation of China [81230051, 81472734, 31170711, 81321003, 30830048]; Beijing Natural Science Foundation [7120002]; 111 Project of the Ministry of Education, Peking University [BMU20120314, BMU20130364]; Leading Academic Discipline Project of Beijing Education Bureau (to H.Z.).

Conflict of interest statement. None declared.

REFERENCES

- Gehring, W.J., Affolter, M. and Burglin, T. (1994) Homeodomain proteins. *Annu. Rev. Biochem.*, **63**, 487–526.
- Apiou, F., Flagiello, D., Cillo, C., Malfoy, B., Poupon, M.F. and Dutrillaux, B. (1996) Fine mapping of human HOX gene clusters. *Cytogen. Cell Genet.*, **73**, 114–115.
- Garcia-Fernandez, J. (2005) The genesis and evolution of homeobox gene clusters. *Nat. Rev. Genet.*, **6**, 881–892.
- Grier, D.G., Thompson, A., Kwasniewska, A., McGonigle, G.J., Halliday, H.L. and Lappin, T.R. (2005) The pathophysiology of HOX genes and their role in cancer. *J. Pathol.*, **205**, 154–171.
- Chen, H. and Sukumar, S. (2003) HOX genes: emerging stars in cancer. *Cancer biology & therapy*, **2**, 524–525.
- Hayashida, T., Takahashi, F., Chiba, N., Brachtel, E., Takahashi, M., Godin-Heymann, N., Gross, K.W., Vivanco, M., Wijendran, V., Shioda, T. *et al.* (2010) HOXB9, a gene overexpressed in breast cancer, promotes tumorigenicity and lung metastasis. *Proc. Natl. Acad. Sci. U.S.A.*, **107**, 1100–1105.
- Abate-Shen, C. (2002) Deregulated homeobox gene expression in cancer: cause or consequence? *Nat. Rev. Cancer*, **2**, 777–785.
- Rhoads, K., Arderiu, G., Charboneau, A., Hansen, S.L., Hoffman, W. and Boudreau, N. (2005) A role for Hox A5 in regulating angiogenesis and vascular patterning. *Lymphatic Res. Biol.*, **3**, 240–252.
- Fromental-Ramain, C., Warot, X., Lakkaraju, S., Favier, B., Haack, H., Birling, C., Dierich, A., Dollé, P. and Chambon, P. (1996) Specific and redundant functions of the paralogous Hoxa-9 and Hoxd-9 genes in forelimb and axial skeleton patterning. *Development*, **122**, 461–472.
- Chen, F. and Capecchi, M.R. (1999) Paralogous mouse Hox genes, Hoxa9, Hoxb9, and Hoxd9, function together to control development of the mammary gland in response to pregnancy. *Proc. Natl. Acad. Sci. U.S.A.*, **96**, 541–546.
- Chiba, N., Comaillès, V., Shiotani, B., Takahashi, F., Shimada, T., Tajima, K., Winokur, D., Hayashida, T., Willers, H., Brachtel, E. *et al.* (2012) Homeobox B9 induces epithelial-to-mesenchymal transition-associated radioresistance by accelerating DNA damage responses. *Proc. Natl. Acad. Sci. U.S.A.*, **109**, 2760–2765.
- Shrestha, B., Ansari, K.I., Bhan, A., Kasiri, S., Hussain, I. and Mandal, S.S. (2012) Homeodomain-containing protein HOXB9 regulates expression of growth and angiogenic factors, facilitates tumor growth *in vitro* and is overexpressed in breast cancer tissue. *FEBS J.*, **279**, 3715–3726.
- Zhan, J., Wang, P., Niu, M., Wang, Y., Zhu, X., Guo, Y. and Zhang, H. (2015) High expression of transcriptional factor HoxB9 predicts poor prognosis in patients with lung adenocarcinoma. *Histopathology*, **66**, 955–965.
- Zhan, J., Niu, M., Wang, P., Zhu, X., Li, S., Song, J., He, H., Wang, Y., Xue, L., Fang, W. *et al.* (2014) Elevated HOXB9 expression promotes differentiation and predicts a favourable outcome in colon adenocarcinoma patients. *Br. J. Cancer*, **111**, 883–893.
- Sha, S., Gu, Y., Xu, B., Hu, H., Yang, Y., Kong, X. and Wu, K. (2013) Decreased expression of HOXB9 is related to poor overall survival in patients with gastric carcinoma. *Digest. Liver Dis.*, **45**, 422–429.
- Chang, Q., Zhang, L., He, C., Zhang, B., Zhang, J., Liu, B., Zeng, N. and Zhu, Z. (2015) HOXB9 induction of mesenchymal-to-epithelial transition in gastric carcinoma is negatively regulated by its hexapeptide motif. *Oncotarget.*, **6**, 42838–42853.
- Zhan, J., Song, J., Wang, P., Chi, X., Wang, Y., Guo, Y., Fang, W. and Zhang, H. (2015) Kindlin-2 induced by TGF- β signaling promotes pancreatic ductal adenocarcinoma progression through downregulation of transcriptional factor HOXB9. *Cancer Lett.*, **361**, 75–85.
- Nagel, S., Burek, C., Venturini, L., Scherr, M., Quentmeier, H., Meyer, C., Rosenwald, A., Drexler, H.G. and MacLeod, R.A. (2007) Comprehensive analysis of homeobox genes in Hodgkin lymphoma cell lines identifies dysregulated expression of HOXB9 mediated via ERK5 signaling and BMI1. *Blood*, **109**, 3015–3023.
- Nguyen, D.X., Chiang, A.C., Zhang, X.H., Kim, J.Y., Kris, M.G., Ladanyi, M., Gerald, W.L. and Massague, J. (2009) WNT/TCF signaling through LEF1 and HOXB9 mediates lung adenocarcinoma metastasis. *Cell*, **138**, 51–62.
- Zhussupova, A., Hayashida, T., Takahashi, M., Miyao, K., Okazaki, H., Jinno, H. and Kitagawa, Y. (2014) An E2F1-HOXB9 transcriptional circuit is associated with breast cancer progression. *PLoS One*, **9**, e105285.
- Yuan, R., Wang, K., Hu, J., Yan, C., Li, M., Yu, X., Liu, X., Lei, J., Guo, W., Wu, L. *et al.* (2014) Ubiquitin-like protein FAT10 promotes the invasion and metastasis of hepatocellular carcinoma by modifying beta-catenin degradation. *Cancer Res.*, **74**, 5287–5300.
- Latham, J.A. and Dent, S.Y. (2007) Cross-regulation of histone modifications. *Nat. Struct. Mol. Biol.*, **14**, 1017–1024.
- Yang, X.J. and Seto, E. (2008) Lysine acetylation: codified crosstalk with other posttranslational modifications. *Mol. Cell*, **31**, 449–461.

24. Jiang, L., Kon, N., Li, T., Wang, S.J., Su, T., Hibshoosh, H., Baer, R. and Gu, W. (2015) Ferroptosis as a p53-mediated activity during tumour suppression. *Nature*, **520**, 57–62.
25. Yuan, Z.L., Guan, Y.J., Chatterjee, D. and Chin, Y.E. (2005) Stat3 dimerization regulated by reversible acetylation of a single lysine residue. *Science*, **307**, 269–273.
26. Kruse, J.P. and Gu, W. (2008) SnapShot: p53 posttranslational modifications. *Cell*, **133**, 930–930.
27. Wan, J., Zhan, J., Li, S., Ma, J., Xu, W., Liu, C., Xue, X., Xie, Y., Fang, W., Chin, Y.E. *et al.* (2015) PCAF-primed EZH2 acetylation regulates its stability and promotes lung adenocarcinoma progression. *Nucleic Acids Res.*, **43**, 3591–3604.
28. Dai, C. and Gu, W. (2010) p53 post-translational modification: deregulated in tumorigenesis. *Trends Mol. Med.* **16**, 528–536.
29. Kim, J.H., Kim, Y.H., Han, J.H., Lee, K.B., Sheen, S.S., Lee, J., Soh, E.Y. and Park, T.J. (2012) Silencing of homeobox B9 is associated with down-regulation of CD56 and extrathyroidal extension of tumor in papillary thyroid carcinoma. *Hum. Pathol.*, **43**, 1221–1228.
30. Chang, B., Chen, Y., Zhao, Y. and Bruick, R.K. (2007) JMJD6 is a histone arginine demethylase. *Science*, **318**, 444–447.
31. Wang, F., He, L., Huangyang, P., Liang, J., Si, W., Yan, R., Han, X., Liu, S., Gui, B., Li, W. *et al.* (2014) JMJD6 promotes colon carcinogenesis through negative regulation of p53 by hydroxylation. *PLoS Biol.*, **12**, e1001819.
32. Zhang, J., Ni, S.S., Zhao, W.L., Dong, X.C. and Wang, J.L. (2013) High expression of JMJD6 predicts unfavorable survival in lung adenocarcinoma. *Tumour Biol.*, **34**, 2397–2401.
33. Lee, Y.F., Miller, L.D., Chan, X.B., Black, M.A., Pang, B., Ong, C.W., Salto-Tellez, M., Liu, E.T. and Desai, K.V. (2012) JMJD6 is a driver of cellular proliferation and motility and a marker of poor prognosis in breast cancer. *Breast Cancer Res.: BCR*, **14**, R85.
34. Klose, R.J., Kallin, E.M. and Zhang, Y. (2006) JmjC-domain-containing proteins and histone demethylation. *Nat. Rev. Genet.*, **7**, 715–727.
35. Liu, W., Ma, Q., Wong, K., Li, W., Ohgi, K., Zhang, J., Aggarwal, A.K. and Rosenfeld, M.G. (2013) Brd4 and JMJD6-associated anti-pause enhancers in regulation of transcriptional pause release. *Cell*, **155**, 1581–1595.
36. Webby, C.J., Wolf, A., Gromak, N., Dreger, M., Kramer, H., Kessler, B., Nielsen, M.L., Schmitz, C., Butler, D.S., Yates, J.R. 3rd *et al.* (2009) Jmjd6 catalyses lysyl-hydroxylation of U2AF65, a protein associated with RNA splicing. *Science*, **325**, 90–93.
37. Boeckel, J.N., Guarani, V., Koyanagi, M., Roex, T., Lengeling, A., Schermuly, R.T., Gellert, P., Braun, T., Zeher, A. and Dimmeler, S. (2011) Jumonji domain-containing protein 6 (Jmjd6) is required for angiogenic sprouting and regulates splicing of VEGF-receptor 1. *Proc. Natl. Acad. Sci. U.S.A.*, **108**, 3276–3281.
38. Unoki, M., Masuda, A., Dohmae, N., Arita, K., Yoshimatsu, M., Iwai, Y., Fukui, Y., Ueda, K., Hamamoto, R., Shirakawa, M. *et al.* (2013) Lysyl 5-hydroxylation, a novel histone modification, by Jumonji domain containing 6 (JMJD6). *J. Biol. Chem.*, **288**, 6053–6062.
39. Bottger, A., Islam, M.S., Chowdhury, R., Schofield, C.J. and Wolf, A. (2015) The oxygenase Jmjd6—a case study in conflicting assignments. *Biochem. J.*, **468**, 191–202.
40. Yanagihara, T., Sanematsu, F., Sato, T., Uruno, T., Duan, X., Tomino, T., Harada, Y., Watanabe, M., Wang, Y., Tanaka, Y. *et al.* (2015) Intronic regulation of Aire expression by Jmjd6 for self-tolerance induction in the thymus. *Nat. Commun.*, **6**, 8820.
41. Subramanian, J. and Govindan, R. (2007) Lung cancer in never smokers: a review. *J. Clin. Oncol.*, **25**, 561–570.
42. Travis, W.D. (2011) Pathology of lung cancer. *Clin. Chest Med.*, **32**, 669–692.
43. Yanagawa, N., Shiono, S., Abiko, M., Ogata, S.Y., Sato, T. and Tamura, G. (2013) New IASLC/ATS/ERS classification and invasive tumor size are predictive of disease recurrence in stage I lung adenocarcinoma. *J. Thoracic Oncol.*, **8**, 612–618.